

# Overview and Comparison of Equalization Schemes for Space-Time-Coded Signals with Application to EDGE

Naofal Al-Dhahir  
AT&T Shannon Laboratory  
Florham Park, NJ 07932  
naofal@research.att.com

**Keywords :** Equalizers, Space-Time Coding, Broadband Wireless, MIMO, EDGE.

## Abstract

This paper describes and compares several practical equalization schemes for space-time-coded transmissions over broadband wireless channels. For space-time trellis codes, we describe and compare two reduced-complexity trellis-based joint equalization and decoding schemes whose performance is further optimized by a front-end FIR channel-shortening prefilter. For space-time block codes, we describe and compare three joint equalization and decoding schemes based on a block-level implementation of the well-known Alamouti scheme either in the time or frequency domains.

We consider the third-generation TDMA cellular system EDGE and recommend a promising equalization scheme for space-time trellis-coded and for Alamouti-type space-time block-coded dual-antenna transmissions based on simulation results for typical urban channel conditions where the delay spread is few symbol periods.

## I. INTRODUCTION

Achieving high bit rates over broadband wireless channels brings the dream of the wireless Internet, and its plethora of interactive multimedia services and applications for users at any place and any time, much closer to reality. Communication theory suggests the following four guidelines for increasing the bit rate

- *Increase the symbol rate* (or equivalently transmission bandwidth) : the price paid is increased susceptibility to intersymbol interference (ISI) and increased processing speed. It is also limited by the scarcity and high-cost of radio frequency (RF) spectrum.

- *Increase signal constellation size* (or equivalently the transmission spectral efficiency) : the price paid is reduced noise immunity (assuming fixed transmitted power) during bad channel conditions (low SNR due to fading) and increased susceptibility to synchronization errors (carrier frequency offsets and phase noise). Error correction coding and adaptive modulation techniques can be used to improve the link margin.
- *Increase transmitted power* : this is undesirable in wireless transmission because it increases non-linear distortion in power amplifiers, reduces battery life at the subscriber terminal, and increases co-channel interference.
- *Use of multiple transmit and/or receive antennas* either to increase *throughput* (by using spatial multiplexing to create multiple parallel channels for transmission of independent information streams) or increase *diversity* level by transmitting correlated replicas of a single information stream (since the probability of simultaneous fading over all transmission channels is small given that antennas are spaced wide enough). The price paid is the cost of implementing multiple RF chains and increased space requirements.

The third-generation TDMA cellular standard known as *Enhanced Data Rates for Global Evolution* (EDGE) [1] achieves a significant bit rate increase over its second-generation predecessors IS-136 and GSM by

- Increasing the symbol rate from 24 Ksymbols/sec in IS-136 to 271 ksymbols/sec.
- Increasing the signal constellation size from DQPSK in IS-136 and (binary) GMSK in GSM to 8-PSK.

As wireless communications systems look to make the transition from voice communications to interactive Internet data, achieving higher bit rates becomes both increasingly desirable and challenging. Space-Time Coding (STC) [2, 3, 4] is a communications technique for wireless systems that employ multiple transmit antennas and single or multiple receive antennas. Space-time codes realize diversity and (possibly) coding gains by introducing temporal and spatial correlation into the signals transmitted from different antennas. Combining EDGE with STC would further increase its achievable bit rate without transmit power increase.

Initial STC research efforts focused on narrowband flat-fading channels [2, 3]. As the transmission bandwidth increases beyond the *coherence bandwidth* [5] of the channel (which is typically defined as the condition for broadband transmission), ISI becomes a major performance-limiting impairment and

equalization becomes indispensable. Equalization complexity increases with the channel memory<sup>1</sup>, signal constellation size, and the use of multiple transmit antennas. This, in turn, places significant additional computational and power consumption loads on user terminals. By virtue of their design, space–time–coded signals have a structure that can be exploited to develop near–optimum reduced–complexity joint equalization and decoding algorithms. The objective of this paper is to present examples of such practical algorithms and compare them for space–time trellis–coded and block–coded transmissions over broadband wireless channels.

Throughout this paper, the EDGE typical urban (TU) channel with 8–PSK modulation will be taken as a case study for two main reasons. First, the EDGE system is currently being deployed as an evolution of second–generation TDMA cellular systems to third generation. Hence, there is great interest in evaluating its performance under a variety of practical operating conditions including the benefits of STC transmissions using two transmit antennas at the base station in a typical urban environment. Second, equalization for EDGE is a challenging problem due to the use of 8–PSK modulation (as opposed to binary modulation used in GSM) and the generally non minimum–phase characteristics of the TU channel impulse response and the additional ISI due to the Gaussian minimum shift keying (GMSK) transmit filter. We emphasize that the equalization schemes presented in this paper are not restricted to the EDGE environment or 8–PSK modulation but apply to other signal constellations and ISI channels.

The main contribution of this paper is a description and comparison of promising practical state–of–the–art joint equalization and decoding schemes for some space–time trellis and block codes. Simulation results comparing the performance of these schemes in a TU EDGE environment are presented and analyzed to recommend a joint equalization and decoding scheme for STC transmission over EDGE. A special effort has been made to provide a comprehensive and up–to–date reference list to aid the interested reader in a further investigation of any of the discussed topics. To the best of this author’s knowledge, no such study exists in the literature at the time of this writing. This has motivated us to write this paper especially since STC technology has been adopted in several third–generation wireless standards and is being considered for fourth–generation standards.

The rest of this paper is organized as follows. We start in Section II by describing the channel model and assumptions. Then, we give a brief overview of STC techniques. In Section III, candidate space–time equalization schemes are described and their pros and cons delineated. This is followed by a discussion of channel estimation issues for space–time–coded systems in Section IV. Simulation results are given in Section V for the EDGE environment and the paper is concluded in Section VI.

---

<sup>1</sup>For a given channel time delay spread [5], the channel memory increases linearly with the transmission bandwidth.

## II. BACKGROUND

### II-A. Channel Model and Assumptions

We consider space–time–coded signaling over frequency–selective channels where a single information stream is mapped by a space–time encoder to  $n_i$  streams. These streams are transmitted simultaneously from  $n_i$  antennas and received by  $n_o$  antennas. We focus on the case  $n_i = 2$  and  $n_o = 1$  in this paper for the following reasons. First, from the user terminal’s perspective, it is the most practical architecture for the downlink to reduce the size and complexity of the user terminal. Second, from the base station’s perspective, substantial diversity gains are realized when going from one to two transmit antennas; less gains in going from two to three transmit antennas and so on (diminishing returns) while the joint equalization and decoding complexity for space–time trellis codes continues to rise exponentially with the number of transmit antennas. Therefore, having two transmit antennas at the base station achieves a favorable performance–complexity tradeoff and makes good engineering sense. Third, for space–time block codes, the case of more than two transmit antennas can be accommodated using the theory of *orthogonal designs* (see [6] for the flat–fading case and the recent paper [7] for an extension to ISI channels). It is this author’s opinion that, for an overview paper of joint space–time equalization and decoding schemes, the case  $n_i = 2$  and  $n_o = 1$  conveys the main concepts without unduly complicating the presentation.

The channel impulse response (CIR) from the  $i^{th}$  transmit antenna to the receive antenna is modeled as a finite–impulse–response (FIR) filter with memory  $\nu$  and denoted by the vector  $\mathbf{h}_i$  or its corresponding D–transform  $h_i(D) \stackrel{def}{=} \sum_{k=0}^{\nu} \mathbf{h}_i(k)D^k$ .<sup>2</sup> The two CIRs are assumed constant over the transmission block (quasi–static fading), independent of each other<sup>3</sup>, and vary independently from block to block. The transmitted symbols are assumed complex zero–mean and belong to a size– $2^b$  standard signal constellation. All of the examples and illustrations in this paper will be for the 8–PSK constellation adopted in the EDGE standard. The noise is additive white Gaussian and independent of the input. Throughout this paper, we shall use the terms frequency–selective channel, broadband channel, and ISI channel interchangeably.

### II-B. Space-Time Coding

Space–time coding has received considerable attention in academic and industrial circles due to its many advantages. First, it improves the downlink performance (which is the bottleneck in asymmetric

---

<sup>2</sup> $D$  stands for unit delay. The  $D$ –transform is related to the  $Z$ –transform by the mapping  $D = Z^{-1}$ .

<sup>3</sup>This can be achieved in practice by placing the two transmit antennas sufficiently apart.

applications such as Internet browsing and downloading) without the need for multiple receive antennas at the terminals (which are required to have low cost and a small form factor). Second, it can be elegantly combined with channel coding, as shown in [2], realizing a coding gain in addition to the diversity gain. Third, they do not require channel state information (CSI) at the transmitter, i.e. operate in open-loop mode, thus eliminating the need for an expensive and, in case of rapid channel fading, unreliable reverse link. Finally, they have been shown to be robust against non-ideal operating conditions such as antenna correlation, channel estimation errors, and Doppler effects [8, 9]. STCs are divided into two main categories : trellis and block, as described next.

### II-B.1 SPACE-TIME TRELLIS CODES (STTC)

The space-time trellis encoder maps the information bit stream into  $n_i$  streams of symbols (each belonging in a size- $2^b$  signal constellation) that are transmitted simultaneously<sup>4</sup>. STTC design criteria were given in [2] that guarantee full spatial diversity and achieve an additional coding gain on a flat quasi-static fading channel.

As an example, we consider the 8-state 8-PSK STTC for two transmit antennas introduced in [2] whose trellis description is given in Figure 1, where the edge label  $xy$  means that symbol  $x$  is transmitted from the first antenna and symbol  $y$  from the second antenna. The different symbol pairs in a given row label the transitions out of a given state, in order, from top to bottom. An equivalent and convenient (for reasons to become clear shortly) implementation of the 8-state 8-PSK STTC encoder is depicted in Figure 2. This equivalent implementation clearly shows that the 8-state 8-PSK STTC is identical to classical delay diversity transmission [10] *except* that the delayed symbol from the second antenna is multiplied by  $-1$  if it is an odd symbol, i.e.  $\in \{1, 3, 5, 7\}$ . This slight modification results in additional coding gain over a flat-fading channel.

When implementing this STTC over a frequency-selective channel, its structure can be exploited to reduce the complexity of joint equalization and decoding. This is achieved by embedding the space-time encoder in Figure 2 in the two channels  $\mathbf{h}_1$  and  $\mathbf{h}_2$  resulting in an equivalent single-input single-output (SISO) data-dependent CIR with memory  $(\nu + 1)$  whose D-transform is given by

$$\begin{aligned} h_{equiv}^{STTC}(k, D) &= \mathbf{h}_1(0) + \sum_{m=1}^{\nu} (\mathbf{h}_1(m) + p_k \mathbf{h}_2(m-1)) D^m + p_k \mathbf{h}_2(\nu) D^{\nu+1} \\ &= h_1(D) + p_k D h_2(D), \end{aligned} \quad (1)$$

where  $p_k = \pm 1$  is data-dependent. Therefore, trellis-based joint space-time equalization and decoding

---

<sup>4</sup>The total transmitted power is divided equally among the  $n_i$  transmit antennas.

with  $8^{\nu+1}$  states can be performed on this equivalent channel. Without exploiting the STTC structure, trellis equalization requires  $8^{2\nu}$  states and STTC decoding requires 8 states.

## II-B.2 ALAMOUTI-TYPE SPACE-TIME BLOCK CODES (STBC)

The decoding complexity of STTC (measured by the number of trellis states at the decoder) increases exponentially as a function of the diversity level and transmission rate [2]. In addressing the issue of decoding complexity, Alamouti [3] discovered an ingenious space-time block coding scheme for transmission with two antennas. According to this scheme, input symbols are grouped in pairs where symbols  $x_k$  and  $x_{k+1}$  are transmitted at time  $k$  from the first and second antennas, respectively. Then, at time  $k+1$ , symbol  $-\bar{x}_{k+1}$  is transmitted from the first antenna and symbol  $\bar{x}_k$  is transmitted from the second antenna, where  $\bar{(\cdot)}$  denotes complex conjugation. This imposes an orthogonal spatio-temporal structure on the transmitted symbols. Alamouti's STBC has been adopted in several wireless standards such as WCDMA [11] and CDMA2000 [12] due to its many attractive features including the following

- It achieves full diversity at full transmission rate for any (real or complex) signal constellation.
- It does not require CSI at the transmitter (i.e. open loop).
- Maximum likelihood decoding involves only *linear* processing at the receiver (due to the orthogonal code structure).

The main drawbacks of Alamouti's STBC are

- Unlike space-time trellis codes, it does not provide any coding gain.
- A rate-1 STBC cannot be constructed for complex signal constellations with more than two transmit antennas [13].
- The simple decoding rule is valid only for a flat-fading channel where the channel gain is constant over two consecutive symbols. Recently, STBCs have been extended to the frequency-selective channel case by implementing the Alamouti orthogonal signaling scheme at a *block* level instead of *symbol* level (see Subsection III-B).

## III. EQUALIZATION FOR SPACE-TIME CODES

In this section, we describe several state-of-the-art joint equalization and decoding schemes investigated at AT&T Shannon Laboratory over the past two years for space-time-coded signaling over EDGE.

### III-A. Equalization Schemes for Space-Time Trellis Codes

In this section, we describe two reduced-complexity joint equalization and decoding schemes for STTC. In both schemes, an FIR channel-shortening prefilter is used as a front end, hence, we start by describing it.

#### III-A.1 FRONT-END PREFILTER

The objective of the prefilter is to shorten and shape the effective CIR seen by the equalizer to reduce its complexity (since the number of equalizer trellis states is exponential in the CIR memory) and/or optimize its performance (by converting the CIR to a near minimum-phase response). In general, it is not possible for a single prefilter (c.f. Figure 3) to convert both channels  $\mathbf{h}_1$  and  $\mathbf{h}_2$  to become exactly minimum phase as in the SISO case [14]. Alternatively, we can also see from Equation (1) that the equivalent SISO channel for the 8-State 8-PSK STTC is data-dependent and hence time-varying from symbol to symbol which makes it impossible for a single time-invariant prefilter to convert it to minimum phase. The approach taken in [15] was to design the prefilter for the *average* channel assuming that  $p_k$  in Equation (1) assumes the values  $+1$  and  $-1$  with equal probability.

First, we describe the prefilter design problem for a time-invariant channel with memory  $\nu$  and then extend it to the data-dependent time-varying channel case. Assume that the FIR prefilter has  $N_f$  taps and denote its impulse response by the vector  $\mathbf{w}$ . Then, the impulse response of the effective channel at the output of the prefilter is given by  $\mathbf{h}_{eff} = \mathbf{H}\mathbf{w}$  where  $\mathbf{H}$  is the  $(N_f + \nu) \times N_f$  Toeplitz convolution matrix. Let the vector  $\mathbf{h}_{win}$  contain the  $(N_b + 1)$  taps (where  $N_b < \nu$ ) of  $\mathbf{h}_{eff}$  to retain after shortening (whose energy is to be maximized) and let  $\mathbf{h}_{wall}$  contain the remaining taps (whose energy is to be minimized). Then,

$$\mathbf{h}_{win} = \mathbf{J}_{win}\mathbf{h}_{eff} = \underbrace{\mathbf{J}_{win}\mathbf{H}}_{\mathbf{H}_{win}}\mathbf{w} = \mathbf{H}_{win}\mathbf{w}, \quad (2)$$

where the  $(N_b + 1) \times (N_f + \nu)$ -dimensional matrix  $\mathbf{J}_{win}$  is constructed using columns of the identity matrix corresponding to tap positions of  $\mathbf{h}_{win}$  within  $\mathbf{h}_{eff}$ . Similarly,

$$\mathbf{h}_{wall} = \mathbf{J}_{wall}\mathbf{h}_{eff} = \underbrace{\mathbf{J}_{wall}\mathbf{H}}_{\mathbf{H}_{wall}}\mathbf{w} = \mathbf{H}_{wall}\mathbf{w}, \quad (3)$$

where the  $(N_f + \nu - N_b - 1) \times (N_f + \nu)$ -dimensional matrix  $\mathbf{J}_{wall}$  is constructed from the columns of the identity matrix corresponding to tap positions of  $\mathbf{h}_{wall}$  within  $\mathbf{h}_{eff}$ .

The proposed prefilter design criterion maximizes the shortening signal to noise ratio (SSNR), which is defined as the desired signal energy of the shortened channel contained in  $\mathbf{h}_{win}$  divided by the residual

ISI energy in  $\mathbf{h}_{wall}$  plus the noise energy at the prefilter output. The corresponding optimization problem can be formulated as the following generalized eigenvector problem (see [15] and the references therein)

$$\max_{\mathbf{w}} \mathbf{w}^* \mathbf{B} \mathbf{w} \quad \text{subject to } \mathbf{w}^* \mathbf{A} \mathbf{w} = 1, \quad (4)$$

where  $(\cdot)^*$  denotes the complex-conjugate transpose operation,  $\mathbf{B} = \mathbf{H}_{win}^* \mathbf{H}_{win}$ ,  $\mathbf{A} = \mathbf{H}_{wall}^* \mathbf{H}_{wall} + \mathbf{R}_{zz}$ , and  $\mathbf{R}_{zz}$  is the noise auto-correlation matrix at the prefilter input. The optimal solution  $\mathbf{w}_{opt}$  is given by

$$\mathbf{w}_{opt} = (\mathbf{L}_A)^{-1} \mathbf{u}_{max}, \quad (5)$$

where  $\mathbf{A} = \mathbf{L}_A \mathbf{L}_A^*$  is the Cholesky factorization of the matrix  $\mathbf{A}$  and  $\mathbf{u}_{max}$  is the unit-norm eigenvector of matrix  $(\mathbf{L}_A)^{-1} \mathbf{B} (\mathbf{L}_A)^{-1}$  that corresponds to its largest eigenvalue  $\lambda_{max}$ . The resulting optimal SSNR is given by

$$SSNR_{opt} = \frac{\mathbf{w}_{opt}^* \mathbf{B} \mathbf{w}_{opt}}{\mathbf{w}_{opt}^* \mathbf{A} \mathbf{w}_{opt}} = \lambda_{max}. \quad (6)$$

Equation (5) provides the optimal prefilter for a time-invariant channel. For the 8-State 8-PSK STTC with two transmit antennas, we can design the prefilter for the *average* of the equivalent channel given in (1). It can be shown [15] that the matrices  $\mathbf{A}$  and  $\mathbf{B}$  in this case are modified to

$$\begin{aligned} \mathbf{B} &= (\mathbf{H}_{win}^1)^* \mathbf{H}_{win}^1 + (\mathbf{H}_{win}^2)^* \mathbf{H}_{win}^2 \\ \mathbf{A} &= (\mathbf{H}_{wall}^1)^* \mathbf{H}_{wall}^1 + (\mathbf{H}_{wall}^2)^* \mathbf{H}_{wall}^2 + \mathbf{R}_{zz}, \end{aligned}$$

where  $\mathbf{H}_{win}^i$  and  $\mathbf{H}_{wall}^i$  ( $i = 1, 2$ ) are matrices corresponding to the constant channels  $\mathbf{h}_1$  and  $\mathbf{h}_2$  between the two transmit and the single receive antennas (c.f. Equations (2) and (3)).

To summarize, the main attractive feature of the prefilter is that it is a single time-invariant (over a transmission block) FIR filter that shortens both channels  $\mathbf{h}_1$  and  $\mathbf{h}_2$  simultaneously without excessive noise enhancement.

### III-A.2 PREFILTERED M-BCJR EQUALIZER

The M-BCJR algorithm, proposed in [16], is a reduced-complexity version of the Bahl-Cocke-Jelinek-Raviv (BCJR) forward-backward algorithm [17] where at each trellis step, only the  $M$  active states associated with the highest metrics are retained. An improved version of the M-BCJR algorithm was proposed in [18] based on a log-domain implementation of the BCJR algorithm and operates as follows. The forward and backward recursions independently select trees of active nodes without restricting one to be a subtree of the other. To form soft decisions at any time instant, we use all edges with at least one active node. An algorithmic description of the improved M-BCJR algorithm [18] follows.

Let  $L$  denote the number of trellis steps,  $Y_1 Y_2 \dots Y_L$  the received outputs,  $s_t$  a trellis state at time  $t$ ,  $S$  the number of trellis states, and  $u_t$  the input at time  $t$ . The quantity we calculate is not  $Pr(u_t = u | Y_1 \dots Y_L)$  as in BCJR but an approximation, as detailed below.

- Using the channel observations and the channel description, calculate for each trellis step  $t$  the quantities

$$\gamma_t(i, j) = Pr(s_t = j; Y_t | s_{t-1} = i) . \quad (7)$$

- The forward recursion is given by

1. for  $t = 0$  (initialization)  $\alpha_0(0) = 1$ ,  $\alpha_0(i) = 0$  for  $i = 1 \dots S$ .

2. for  $t = 1, \dots, L - 1$

(a)  $\alpha_t(i) = \sum_j \alpha_{t-1}(j) \gamma_t(i, j)$ .

(b) Let  $A_t$  denote the  $M$  largest  $\alpha$ 's at time  $t$ . Any sorting algorithm can be used to construct  $A_t$ . Set  $\alpha_t(i) = 0$  if  $\alpha_t(i) \notin A_t$ .

- Similarly, the backward recursion is given by

1. for  $t = L$  (initialization)  $\beta_L(0) = 1$ ,  $\beta_L(i) = 0$  for  $i = 1, \dots, S$ .

2. for  $t = L - 1, \dots, 1$

(a)  $\beta_t(i) = \sum_j \beta_{t+1}(j) \gamma_{t+1}(i, j)$ .

(b) Let  $B_t$  denote the  $M$  largest  $\beta$ 's at time  $t$ . Any sorting algorithm can be used to construct  $B_t$ . Set  $\beta_t(i) = 0$  if  $\beta_t(i) \notin B_t$ .

- Calculate the probabilities of error  $E_\alpha$  and  $E_\beta$  (in the sense that the correct state is not included in the  $M$  selected states) as follows

$$E_\alpha = Q(\sqrt{|\mathbf{h}(0)|^2 d_{min}^2 / 2\sigma_z^2}) ; E_\beta = Q(\sqrt{|\mathbf{h}(\nu)|^2 d_{min}^2 / 2\sigma_z^2}) ,$$

where  $Q(\cdot)$  is the standard Q function,  $d_{min}$  is the minimum Euclidean distance between any two constellation points, and  $\sigma_z^2$  is the noise variance.

- To make a decision at step  $0 < t < L$  on the input  $u_t = u$  do

–  $P(u_t = u) = 0$ .

– For all edges  $(i, j)$  that have input  $u$

1. if  $\beta_t(j) \neq 0$  and  $\alpha_{t-1}(i) \neq 0$ , then  $P(u_t = u)^+ = \alpha_{t-1}(i)\gamma(i, j)\beta_t(j)$ .
2. if  $\beta_t(j) \neq 0$  and  $\alpha_{t-1}(i) = 0$ , then  $P(u_t = u)^+ = E_\alpha\gamma(i, j)\beta_t(j)$ .
3. if  $\beta_t(j) = 0$  and  $\alpha_{t-1}(i) \neq 0$ , then  $P(u_t = u)^+ = \alpha_{t-1}(i)\gamma(i, j)E_\beta$ .

The performance of the M-BCJR equalizer/decoder is further improved, especially for small  $M$ , by using the prefilter of the previous subsection to concentrate the channel energy in a small number of taps. In fact, two different prefilters should be used for the forward and backward recursions since the forward recursion favors a close to minimum-phase channel while the backward recursion favors a close to maximum-phase channel [18]. The value of  $M$  and the number of prefilter taps can be jointly optimized to achieve the best performance-complexity tradeoffs.

### III-A.3 PREFILTERED MLSE/DDFSE EQUALIZER

Unlike the BJCR maximum a posteriori (MAP) equalizer [17] which minimizes the *symbol* error probability, maximum likelihood sequence estimation (MLSE) [14] minimizes the *sequence* error probability and can be implemented efficiently using the Viterbi algorithm. A major advantage of the BCJR-MAP algorithm over the conventional Viterbi algorithm<sup>5</sup> is the generation of *soft* information on the decisions. Generalization of the MLSE equalizer to the multiple-input multiple-output (MIMO) case was first reported by Van Etten [20].

For a size- $2^b$  signal constellation,  $n_i$  transmit antennas, and MIMO channel memory of  $\nu$ <sup>6</sup>, the MIMO MLSE equalizer has  $2^{bn_i\nu}$  states in general. The number of equalizer states can be reduced by using the STTC trellis structure as shown in [21] or by a MIMO channel-shortening prefilter [22]. However, this complexity is still too high for large signal constellations, even for two transmit antennas and short-to-moderate MIMO channel memory. For example, for 8-PSK constellation and the EDGE TU channel (where  $\nu = 3$ ), the number of full MLSE equalizer states is equal to  $8^6 = 262,144$  states.

As a remedy, delayed decision feedback sequence estimation (DDFSE) was introduced in [23] as a hybrid scheme between MLSE and decision feedback equalization (DFE) for channels with long memory. Basically, the CIR is divided into a leading part and a tail. Then, an MLSE equalizer is constructed based on the leading part and the interfering effect of the CIR tail is canceled by feedback using previous (hard) decisions (assumed correct).

---

<sup>5</sup>A modified soft-output Viterbi algorithm (SOVA) was presented in [19]. However, its performance is suboptimal compared to BCJR-MAP.

<sup>6</sup>The memory of a MIMO channel is defined here to be the maximum of the memories of its constituent SISO channels.

At time  $k$ , the branch metric  $\xi(k)$  of the DDFSE equalizer/decoder is given by

$$\xi(k) = \left| y(k) - \sum_{i=0}^n \mathbf{h}_{eqv}^{STTC}(i) x(k-i) - \sum_{i=n+1}^{\nu+1} \mathbf{h}_{eqv}^{STTC}(i) \hat{x}(k-i) \right|^2, \quad (8)$$

where  $y(k)$  is the  $k^{th}$  received symbol,  $n$  is a design parameter ( $0 \leq n \leq \nu$ ) that determines the number of DDFSE trellis states,  $\mathbf{h}_{eqv}^{STTC}$  is the impulse response vector of the equivalent channel (c.f. Equation 1),  $x(k)$  are all possible input symbols according to different transitions along the path history, and  $\hat{x}(k)$  are the previous hard symbol decisions along the path history. DDFSE assumes that these symbols are decoded correctly and uses them to equalize the effect of the discarded trellis states. From (8), we can see that DDFSE can be considered as a combination of MLSE and DFE that uses a state description of the channel to recursively estimate the best path in the trellis while storing only one path for each state as in MLSE. However, in the DDFSE case, each state (which corresponds to  $n$  symbols of channel memory) provides only partial information about the full state of the channel. In order to cancel the interference from the past symbols occurring earlier than  $n$  symbols in the past, hard feedback information is extracted from the best path. Like all feedback schemes, DDFSE suffers from error propagation effects. These effects are minimized if most of the channel energy is concentrated in its leading part.<sup>7</sup> This is the task of the FIR prefilter which minimizes the CIR tail energy.

We conclude this section with the following two remarks. First, other candidate STTC equalization schemes that have been reported in the literature include turbo equalization, OFDM, and linear or decision feedback equalizers are described in [24], [25], [26], and [27]. Additional promising equalization schemes include the T-BCJR [16] and RSSE [28] algorithms. These schemes were not part of our investigation of STC application to EDGE and hence are not covered here. Second, we emphasize that the two equalization schemes described in this section are not limited to 8-PSK constellation or the 8-state STTC with two transmit antennas. They can be applied to other signal constellations and other STTC's as well (see [2] for STTC examples for different constellation sizes and numbers of transmit antennas). The starting point would be the development of an equivalent SISO encoder model for the STTC under consideration (analogous to the model in Figure 2).

### III-B. Equalization Schemes for Space-Time Block Codes

Our focus will be on the case of two transmit antennas where full-rate Alamouti-type space-time block codes can be constructed for any signal constellation.

---

<sup>7</sup>As in minimum-phase channels.

### III-B.1 TIME-REVERSAL SPACE-TIME BLOCK CODING (TR-STBC)

TR-STBC was introduced in [29] as an extension of the Alamouti STBC scheme [3] to frequency-selective channels by imposing the Alamouti orthogonal structure at a *block not symbol* level as in the flat-fading channel case. More specifically, the transmitted blocks from Antennas 1 and 2 at time  $(k+1)$  (denoted by  $\mathbf{x}_1^{(k+1)}$  and  $\mathbf{x}_2^{(k+1)}$ , respectively) are generated by the encoding rule (for  $k = 0, 2, 4, \dots$ )

$$\mathbf{x}_1^{(k+1)} = -\mathbf{J}\bar{\mathbf{x}}_2^{(k)} ; \mathbf{x}_2^{(k+1)} = \mathbf{J}\bar{\mathbf{x}}_1^{(k)} , \quad (9)$$

where  $\mathbf{J}$  is the time-reversal matrix which consists of ones on the main anti-diagonal and zeros everywhere. To eliminate inter-block interference (IBI) between adjacent blocks due to channel memory, length- $\nu$  all-zeros guard sequences are inserted between information blocks.

At the receiver end (c.f. Figure 4), TR-STBC employs linear combining techniques (a spatio-temporal matched filter) to eliminate the mutual interference effects between the two transmit antennas *while still achieving the maximum diversity gain* of  $\|\mathbf{h}_1\|^2 + \|\mathbf{h}_2\|^2$  (where  $\|\cdot\|$  denotes the norm of a vector). Effectively, TR-STBC uses a combination of complex-conjugation, time-reversal, and matched-filtering operations, as described in detail in [29], to convert the two-input single-output channel to two SISO channels each with an equivalent impulse response given by

$$h_{eqv}^{TR-STBC}(D) = h_1(D)\bar{h}_1(\bar{D}^{-1}) + h_2(D)\bar{h}_2(\bar{D}^{-1}) \quad (10)$$

to which standard SISO equalization schemes can be applied [14].<sup>8</sup> For example, a whitened matched filter (WMF) front-end can be used to convert  $h_{eqv}^{TR-STBC}(D)$  to its minimum-phase equivalent<sup>9</sup> followed by trellis or feedback equalization as it will be further discussed in Section V. TR-STBC assumes that the two channels  $h_1(D)$  and  $h_2(D)$  are fixed over two consecutive transmission blocks and perfectly known at the receiver. In the next two subsections, we describe two alternative STBC joint equalization/decoding schemes that use frequency-domain processing.

### III-B.2 ORTHOGONAL FREQUENCY DIVISION MULTIPLEXED SPACE-TIME BLOCK CODING (OFDM-STBC)

In OFDM, the high-rate input stream is demultiplexed and transmitted over  $N$  low-rate independent frequency subcarriers. This multicarrier transmission scheme is implemented digitally using the efficient Fast Fourier Transform (FFT) [30]. Since OFDM is a block transmission scheme, a guard sequence (of

<sup>8</sup>In Equation (10),  $h_i(D)$  is the  $D$ -transform of  $\mathbf{h}_i(k)$  and  $\bar{h}_i(\bar{D}^{-1})$  is the  $D$ -transform of  $\bar{\mathbf{h}}_i(-k)$  for  $i = 1, 2$ .

<sup>9</sup>Unlike the STTC case, exact conversion to minimum phase is possible here since  $h_{eqv}^{TR-STBC}(D)$  is not data-dependent.

length at least equal to channel memory) is needed to eliminate IBI and ensure that individual subcarriers can be isolated at the receiver. The most popular choice for guard sequence is a *cyclic prefix* which makes the channel matrix *circulant*, hence, diagonalizable by the FFT. If the FFT size is made large enough such that the width of each frequency bin is less than the *coherence bandwidth* of the channel, then no equalization is needed<sup>10</sup>. A large FFT size (compared to channel memory) also reduces the cyclic prefix guard sequence overhead at the expense of increased storage and processing requirements and increased delay which might not be acceptable for delay-sensitive applications.

An elegant scheme for combining OFDM and STBC by implementing the Alamouti orthogonal structure at a block level was first reported in [31]. The channel is assumed fixed over two consecutive OFDM blocks and known at the receiver and a cyclic prefix is added to each block to eliminate IBI and render the two channel matrices circulant. Therefore, simultaneous equalization of the two frequency-selective channels  $\mathbf{h}_1$  and  $\mathbf{h}_2$  is achieved by using the computationally-efficient IFFT/FFT modulation/demodulation vectors to divide the spectra of both channels into a large number of parallel independent frequency-flat subchannels. At the receiver end (c.f. Figure 5), received blocks are processed in pairs where their FFTs are computed and linearly combined. Finally, gain and phase adjustment is performed using minimum mean square error frequency-domain equalization (MMSE-FDE) with a single complex tap for each subchannel followed by decision device.

While the use of the Alamouti STBC modifies the channel frequency gain at subchannel  $i$  from  $|H(i)|^2$  to  $|H_1(i)|^2 + |H_2(i)|^2$  which provides increased immunity against fading, decision errors occurring at any subchannel result in an irreducible error floor. As shown in [32], OFDM-STBC cannot fully exploit the multipath diversity gains of the two channels. This limitation can be overcome by frequency interleaving and forward error correction [33] or linear precoding [34].

OFDM offers great flexibility in that multiple signals with different rates and quality-of-service (QoS) requirements can be transmitted over the parallel frequency subchannels. Moreover, avoiding strong RF narrowband interference within the transmission bandwidth is easily accomplished by turning off the corresponding subchannels. On the other hand, OFDM has two main drawbacks, namely a high peak to average ratio (PAR), which results in larger backoff with nonlinear amplifiers [35], and high sensitivity to frequency errors and phase noise [36]. An alternative equalization scheme that overcomes these two drawbacks of OFDM while retaining its reduced implementation complexity advantage (due to use of FFT) is the single-carrier (SC) FDE [33] which has been extended to receive-diversity systems in [37] and to Alamouti-type STBC transmit-diversity systems in [38] and is described in the next subsection.

---

<sup>10</sup>Except for a simple one-tap complex equalizer for each subchannel, assuming negligible inter-carrier interference due to Doppler effects or frequency offset errors.

We conclude this section by emphasizing that the three STBC equalization schemes described above are applicable to any signal constellation (not just 8-PSK) and any FIR channel (not just TU EDGE). These schemes can be extended to more than two transmit antennas using the theory of *orthogonal designs* [6], as done for TR-STBC in [7].

### III-B.3 SINGLE-CARRIER FREQUENCY-DOMAIN EQUALIZED SPACE-TIME BLOCK CODING (SC FDE-STBC)

The SC FDE is distinct from OFDM in that the IFFT block is moved to the receiver end and placed before the decision device (c.f. Figure 6). As noted in [33], this causes the effects of deep nulls in the channel frequency response to be spread out, by the IFFT operation, over all symbols thus reducing their effect and improving performance.

Denote the  $n^{\text{th}}$  symbol of the  $k^{\text{th}}$  transmitted block (of length  $N$ ) from antenna  $i$  by  $\mathbf{x}_i^{(k)}(n)$ . Then, the FDE-STBC encoding rule is given by [38]

$$\mathbf{x}_1^{(k+1)}(n) = -\bar{\mathbf{x}}_2^{(k)}((-n)_N) ; \mathbf{x}_2^{(k+1)}(n) = \bar{\mathbf{x}}_1^{(k)}((-n)_N) \quad (11)$$

$$\text{for } n = 0, 1, \dots, N-1 \text{ and } k = 0, 2, 4, \dots$$

where  $(\cdot)_N$  denotes the modulo- $N$  operation which distinguishes this encoding scheme from TR-STBC (c.f. Equation (9)). In addition, a cyclic prefix (CP) is added to each transmitted block to eliminate IBI and make the two channel matrices circulant. Taking the Discrete Fourier Transform (DFT) of (11), we see

$$\mathbf{X}_1^{(k+1)}(m) = -\bar{\mathbf{X}}_2^{(k)}(m) ; \mathbf{X}_2^{(k+1)}(m) = \bar{\mathbf{X}}_1^{(k)}(m) \quad (12)$$

$$\text{for } m = 0, 1, \dots, N-1 \text{ and } k = 0, 2, 4, \dots$$

which reveals that this, too, is a *block-level* implementation of the symbol-level Alamouti encoding rule.

The SC FDE-STBC receiver block diagram is given in Figure 6. After analog-to-digital (A/D) conversion, the CP part of each received block is discarded. Mathematically, we can express the input-output relationship over the  $j^{\text{th}}$  received block as follows

$$\mathbf{y}^{(j)} = \mathbf{H}_1^{(j)} \mathbf{x}_1^{(j)} + \mathbf{H}_2^{(j)} \mathbf{x}_2^{(j)} + \mathbf{z}^{(j)} , \quad (13)$$

where  $\mathbf{H}_1^{(j)}$  and  $\mathbf{H}_2^{(j)}$  are  $N \times N$  circulant matrices whose first columns are equal to  $\mathbf{h}_1^{(j)}$  and  $\mathbf{h}_2^{(j)}$ , respectively, appended by  $(N - \nu - 1)$  zeros and  $\mathbf{z}^{(j)}$  is the noise vector. Since  $\mathbf{H}_1^{(j)}$  and  $\mathbf{H}_2^{(j)}$  are circulant matrices, they admit the eigen-decompositions

$$\mathbf{H}_1^{(j)} = \mathbf{Q}^* \mathbf{\Lambda}_1^{(j)} \mathbf{Q} \quad ; \quad \mathbf{H}_2^{(j)} = \mathbf{Q}^* \mathbf{\Lambda}_2^{(j)} \mathbf{Q} ,$$

where  $\mathbf{Q}$  is the orthonormal FFT matrix and  $\mathbf{\Lambda}_1^{(j)}$  (resp.  $\mathbf{\Lambda}_2^{(j)}$ ) is a diagonal matrix whose  $(n, n)$  entry is equal to the  $n^{\text{th}}$  FFT coefficient of  $\mathbf{h}_1^{(j)}$  (resp.  $\mathbf{h}_2^{(j)}$ ). Therefore, applying the FFT to  $\mathbf{y}^{(j)}$ , we get (for  $j = k, k + 1$ )

$$\mathbf{Y}^{(j)} = \mathbf{Q}\mathbf{y}^{(j)} = \mathbf{\Lambda}_1^{(j)}\mathbf{X}_1^{(j)} + \mathbf{\Lambda}_2^{(j)}\mathbf{X}_2^{(j)} + \mathbf{Z}^{(j)}.$$

The length- $N$  blocks at the FFT output are then processed in pairs resulting in the two blocks (we drop the time index from the channel matrices since they are assumed fixed over the two blocks under consideration)

$$\underbrace{\begin{bmatrix} \mathbf{Y}^{(k)} \\ \bar{\mathbf{Y}}^{(k+1)} \end{bmatrix}}_{\mathbf{Y}} = \underbrace{\begin{bmatrix} \mathbf{\Lambda}_1 & \mathbf{\Lambda}_2 \\ \bar{\mathbf{\Lambda}}_2 & -\bar{\mathbf{\Lambda}}_1 \end{bmatrix}}_{\mathbf{\Lambda}} \underbrace{\begin{bmatrix} \mathbf{X}_1^{(k)} \\ \mathbf{X}_2^{(k)} \end{bmatrix}}_{\mathbf{X}} + \underbrace{\begin{bmatrix} \mathbf{Z}^{(k)} \\ \bar{\mathbf{Z}}^{(k+1)} \end{bmatrix}}_{\mathbf{Z}}, \quad (14)$$

where  $\mathbf{X}_1^{(k)}$  and  $\mathbf{X}_2^{(k)}$  are the FFTs of the information blocks  $\mathbf{x}_1^{(k)}$  and  $\mathbf{x}_2^{(k)}$ , respectively, and  $\mathbf{Z}$  is the noise vector. To eliminate *inter-antenna interference*, the linear combiner  $\mathbf{\Lambda}^*$  is applied to  $\mathbf{Y}$ . Due to the orthogonal Alamouti-like<sup>11</sup> structure of  $\mathbf{\Lambda}$ , a second-order diversity gain is achieved. Then, the two decoupled blocks at the output of the linear combiner are equalized separately using the MMSE FDE [33] which consists of  $N$  complex taps per block that mitigate *inter-symbol interference*. Finally, the MMSE-FDE output is transformed back to the time domain using the inverse FFT where decisions are made.

Note that the SC MMSE-FDE is equivalent to block MMSE linear equalization [39], hence, its performance can be improved at the expense of increased complexity, by adding a feedback section as discussed in [40].

#### IV. CHANNEL ESTIMATION

STC schemes run open loop which makes them very attractive for wireless transmission. Nevertheless, CSI is still required at the receiver to perform joint equalization/decoding. While *differential* STC schemes for frequency-selective channels have been recently developed [41], they incur a significant performance penalty with respect to coherent techniques and hence are more suitable for rapidly time-varying channels. Since our focus here is on quasi-static fading, we only consider coherent STC processing where CSI is estimated at the receiver using a training sequence embedded in each transmission block.

For single-antenna transmission, the training sequence is only required to have “good” (i.e. impulse-like) auto-correlation properties. However, for the  $n_i$  transmit-antenna scenarios, the  $n_i$  training se-

---

<sup>11</sup>We call any  $2 \times 2$  complex orthogonal matrix of the form  $\begin{bmatrix} c_1 & c_2 \\ \pm\bar{c}_2 & \mp\bar{c}_1 \end{bmatrix}$  Alamouti-like.

quences should, in addition, have “low” (ideally zero) cross-correlation. This property makes the channel estimation problem different for multiple-antenna systems from single-antenna systems.

An obvious transmission scheme that forces the cross-correlation between the  $n_i$  training sequences to zero consists of dividing the training interval into  $n_i$  subintervals where only one antenna is allowed to transmit its training sequence in each subinterval. This scheme has two major drawbacks. First, the PAR is increased which, in turn, increases amplifier nonlinear distortion. Second, the effective training period for each transmit antenna is reduced by a factor of  $n_i$ .

Next, we formulate the channel estimation problem for the 2-transmit 1-receive scenario. The analysis can be easily generalized to multiple transmit/receive antennas.

We transmit two training sequences  $\mathbf{s}_1$  and  $\mathbf{s}_2$  from the first and second antennas simultaneously in synchronized data blocks where each block consists of  $N$  information symbols and  $N_t$  training symbols. For two transmit antennas, the receiver uses the  $2N_t$  known training symbols to estimate the  $2(\nu + 1)$  unknown channel coefficients. The observed training sequence output, that does not have interference from information or preamble symbols, can be expressed as

$$\mathbf{y} = [\mathbf{S}_1 \ \mathbf{S}_2] \begin{bmatrix} \mathbf{h}_1 \\ \mathbf{h}_2 \end{bmatrix} + \mathbf{z} = \mathbf{S}\mathbf{h} + \mathbf{z}, \quad (15)$$

where the column vectors  $\mathbf{y}$  and  $\mathbf{z}$  are of size  $(N_t - \nu)$ ,  $\mathbf{S}_1$  and  $\mathbf{S}_2$  are Toeplitz matrices of size  $(N_t - \nu) \times (\nu + 1)$  that contain training symbols. The MMSE channel estimate, assuming that  $\mathbf{S}$  has full column rank, is given by [42]

$$\hat{\mathbf{h}} = \begin{bmatrix} \hat{\mathbf{h}}_1 \\ \hat{\mathbf{h}}_2 \end{bmatrix} = (\mathbf{S}^* \mathbf{S})^{-1} \mathbf{S}^* \mathbf{y}, \quad (16)$$

where  $(\cdot)^{-1}$  denote the inverse. The channel estimation MSE is defined as

$$MSE = E[(\mathbf{h} - \hat{\mathbf{h}})^*(\mathbf{h} - \hat{\mathbf{h}})] = \sigma_z^2 tr((\mathbf{S}^* \mathbf{S})^{-1}), \quad (17)$$

where we assume white noise with variance  $\sigma_z^2$  and  $tr(\cdot)$  denotes the trace of a matrix. The channel estimation MMSE is equal to

$$MMSE = \frac{\sigma_z^2(\nu + 1)}{(N_t - \nu)}, \quad (18)$$

which is achieved if and only if

$$\mathbf{S}^* \mathbf{S} = \begin{bmatrix} \mathbf{S}_1^* \mathbf{S}_1 & \mathbf{S}_2^* \mathbf{S}_1 \\ \mathbf{S}_1^* \mathbf{S}_2 & \mathbf{S}_2^* \mathbf{S}_2 \end{bmatrix} = (N_t - \nu) \mathbf{I}_{\nu+1}, \quad (19)$$

where  $\mathbf{I}_{\nu+1}$  is the identity matrix of size  $\nu + 1$ . Two optimal training sequences that satisfy (19) have an impulse-like auto-correlation sequence and zero cross-correlation. In this case, computing the channel estimates using (16) reduces to a simple cross-correlation (matrix-vector product).

For implementation purposes (to avoid nonlinear amplifier distortion), it is desirable to use training sequences with constant amplitude. Optimal constant-amplitude training sequences can be constructed from a  $P^{th}$  root-of-unity alphabet  $A_P = \{e^{\frac{i2\pi k}{P}} | k = 0, 1, \dots, P-1\}$  (where  $i = \sqrt{-1}$ ), without constraining the alphabet size  $P$ . Such sequences are the perfect roots-of-unity sequences (PRUS), also known as polyphase sequences. Chu [43] showed that for any training sequence length  $N_t$  there exists a PRUS with alphabet size  $P = 2N_t$ . In the next section, we show the effect of channel estimation using PRUS on the performance of STTC and STBC equalizers. We conclude this section by mentioning that, in general, PRUS do not belong to standard signal constellations (e.g. PSK). We showed in [44] and [45] how to design PSK-type training sequences for dual-antenna transmissions with negligible performance loss from PRUS.

## V. SIMULATION RESULTS

### V-A. Simulation Environment

In our simulation results, we consider 8-PSK modulation with two transmit and one receive antennas on the TU EDGE channel. The overall CIR <sup>12</sup> length is effectively four symbol periods; i.e.,  $\nu = 3$ . Therefore, the transmitted signal experiences frequency-selective fading and equalization is needed at the receiver.

In EDGE, fading can be safely assumed to be quasi-static, i.e., the CIR can be assumed constant for the duration of a transmission block. This is due to the fact that the coherence time of the channel at around 1 GHz carrier frequency is much larger than the block duration of  $577\mu sec$  even for highway speeds. This eliminates the need for channel tracking at the receiver. In addition, the fading process is independent from block to block assuming ideal frequency hopping. In our simulations, the noise samples are generated as independent samples of a zero-mean complex Gaussian random variable with a variance of  $\frac{1}{SNR}$  per complex dimension. The reason for doubling the noise variance (compared to the single-transmit-antenna case) is that with two-antenna transmissions, we assume that the total transmitted power is the same as in the single-antenna case and is divided equally between the two antennas. The average energy of the symbols transmitted from each antenna is normalized to one so that the signal to

---

<sup>12</sup>Overall CIR is the convolution of the linearized GMSK transmit filter and the physical multipath channel.

noise ratio is SNR.

### V-B. Bit Error Rate (BER) Results

#### Equalization of STTC

For the 8-state 8-PSK STTC, we show in Figure 7 the performance of the prefiltered M-BCJR equalizer as a function of the number of active states  $M$ . Both channels are shortened to three taps, hence, the maximum value of  $M$  with the prefilter is  $8^3 = 512$  states. Also shown in the figure as a benchmark is the BER of a full BCJR-MAP equalizer with 4096 states<sup>13</sup> and no prefilter. It can be seen that negligible performance improvement is achieved by increasing  $M$  from 16 to its maximum value of 512 due the effective action of the prefilter which concentrates most of the channel energy in its leading or last taps for the forward and backward recursions, respectively. The performance gap from the 4096-state BCJR-MAP is due to the prefilter loss but, in return, we achieve a significant reduction in the number of equalizer/decoder states (from 4096 to 16). Next, we assume a 16-state prefiltered M-BCJR equalizer and compare its performance in Figure 8 with that of a prefiltered DDFSE equalizer and the full BCJR-MAP equalizer. Although the simulated M-BCJR equalizer has less complexity than the DDFSE equalizer (the former has  $M=16$  states and two prefilters each with 8 taps while the latter has 64 states and a single 32-tap prefilter), it performs better for the whole SNR range shown. Moreover, the performance loss of the prefiltered 16-state M-BCJR equalizer from the 4096-state BCJR-MAP equalizer (without prefilter) is less than 3 dB which makes it an attractive joint equalization/decoding scheme for STTC in terms of its performance-complexity tradeoff. The effect of channel estimation errors on its performance is depicted in Figure 9 where a loss of 1–1.5 dB is observed over the entire SNR range considered. For this simulation, we used length-26 PRUS for training and a least squares algorithm (c.f. Equation (16)) to estimate the two channels.

In summary, we propose the M-BCJR with  $M = 16$  states preceded by an 8-tap prefilter as a joint equalization/decoding scheme for the 8-state 8-PSK STTC with two transmit antennas over EDGE for the following reasons. First, it achieves near-optimum performance (e.g. less than 2 dB loss from full BCJR-MAP at  $\text{BER}=10^{-3}$ ) by exploiting the available spatial and multipath diversities. Second, its complexity level is comparable to the 16-state Viterbi equalizer used in current GSM cellular phones. Third, it generates soft information which can be used to enhance the performance of an outer code.

---

<sup>13</sup>The equivalent SISO channel of the 8-state 8-PSK STTC has memory of  $\nu + 1 = 4$  (c.f. Equation (1)). Hence, the number of BCJR-MAP equalizers states is  $8^4 = 4096$ .

### Equalization of STBC

In Figure 10, we compare the performance of the three STBC equalization schemes described in Section III–B. For TR–STBC, the SISO equalizer structure assumed at the receiver (c.f. Figure 4) is the MMSE–DFE with ideal feedforward filter (i.e. WMF) [46] and  $N_b = \nu = 3$  feedback filter taps. For our simulation scenario, we found that a 20–tap FIR implementation of the WMF results in negligible performance loss from the ideal (i.e. infinite–length) WMF. For FDE–STBC and OFDM–STBC, the FFT size used is  $N = 64$ .<sup>14</sup> It can be seen from the figure that even with a suboptimum equalizer like a DFE, TR–STBC outperforms the two other schemes. When OFDM–STBC is combined with frequency–domain interleaving and forward error correction or precoding [34] and a feedback section is added to FDE–STBC, the three schemes exhibit comparable performance. Figure 11<sup>15</sup> shows that PRUS–based channel estimation degrades the performance of SC FDE–STBC by  $\approx 1 - 1.5$  dB. Similar channel estimation sensitivities were observed for OFDM–STBC and TR–STBC. Finally, we investigate the use of more sophisticated equalization schemes to further enhance the performance of TR–STBC. Figure 12 shows the performance of TR–STBC with a 3–tap DFE, an 8–state M–BCJR, and a full 512–state BCJR–MAP equalizers, assuming a WMF front–end that converts  $h_{eqv}^{TR-STBC}(D)$ , as defined in (10), to its minimum–phase equivalent [14]. It is clear from the figure that the 8–state M–BCJR equalizer achieves almost the same performance as the 512–state BCJR–MAP equalizer. This is due to the fact that most of the equivalent channel energy (after WMF) is concentrated in its first two taps. This also makes suboptimum equalization schemes like a DFE with three feedback taps achieve near–optimum performance. Another interesting observation can be made by comparing the performance of equalized STTC and TR–STBC given in Figures 8 and 12, respectively. At a given complexity level, suboptimum equalization schemes (like the 8–state prefiltered M–BCJR) achieve better performance for TR–STBC than for the 8–state 8–PSK STTC since more energy is concentrated in the first two taps of its equivalent channel (after WMF). As explained in Section III, the prefilter of STTC is designed for the average of the  $\mathbf{h}_1$  and  $\mathbf{h}_2$  channels since  $h_{eqv}^{STTC}(k, D)$  is data–dependent and cannot be converted exactly to minimum phase using a single prefilter unlike the case of TR–STBC (c.f. Equation (10)). In summary, our results suggest that TR–STBC combined with an 8–state M–BCJR equalizer achieves the best performance–complexity tradeoff as a space–time coding scheme over the TU EDGE channel with 8–PSK modulation, two transmit antennas, and one receive antenna.

<sup>14</sup>Note that FDE–STBC and OFDM–STBC suffer an additional SNR penalty due to the cyclic prefix. For our simulation parameters, this SNR loss is equal to  $-10 \log_{10} \frac{N}{N+\nu} = -10 \log_{10} \frac{64}{67} = 0.2$  dB.

<sup>15</sup>Note that the horizontal axis in this figure is  $\frac{E_b}{N_0}$  which (for the 8–PSK modulation assumed) is related to the SNR measure used in the other figures by the relation (in dB scale) :  $SNR = \frac{E_b}{N_0} + 4.77$ .

## VI. CONCLUSIONS

In this paper, we discussed the pros and cons of several joint equalization and decoding schemes for space-time trellis- and block-coded transmissions over broadband wireless channels. Based on simulation results of a 2-transmit 1-receive antenna downlink architecture with independent fadings between the two channels, 8-PSK modulation, and typical urban channel conditions, we summarize our findings as follows. For space-time trellis codes, the prefiltered M-BCJR equalizer/decoder outperforms the prefiltered DDFSE equalizer/decoder and has lower implementation complexity. For space-time block codes, TR-STBC achieves the best performance among the three investigated schemes. OFDM-STBC has the highest PAR and is the most sensitive to frequency errors but is also the most flexible among the three schemes in its support of multi-rate and multi-QoS requirements. The three STBC schemes suffer the same amount of overhead (in the form of an all-zeros guard sequence for TR-STBC and a cyclic prefix guard sequence for FDE-STBC and OFDM-STBC). Tables I and II present a performance/complexity comparison summary between all joint equalization/decoding schemes investigated in this paper for STTC and STBC, respectively. Exploiting the structure of space-time codes is critical in developing near-optimum reduced-complexity joint equalization/decoding algorithms.

### Acknowledgement

I would like to thank the following colleagues (in alphabetical order) for many technical discussions and contributions to this work : G. Bauch, A.R. Calderbank, S.N. Diggavi, C. Fragouli, G.B. Giannakis, R. Jana, A.F. Naguib, A.H. Sayed, A. Stamoulis, W. Turin, M. Uysal, and W. Younis. I am also indebted to the anonymous reviewers for their valuable feedback which improved the clarity of the presentation.

## REFERENCES

- [1] A. Furuskar, S. Mazur, F. Muller, and H. Olofsson. EDGE : Enhanced Data Rates for GSM and TDMA/136 Evolution. *IEEE Personal Communications Magazine*, pages 56–66, June 1999.
- [2] V. Tarokh, N. Seshadri, and A.R. Calderbank. Space-Time Codes for High Data Rate Wireless Communications : Performance Criterion and Code Construction. *IEEE Transactions on Information Theory*, pages 744–765, March 1998.
- [3] S. Alamouti. A Simple Transmit Diversity Technique for Wireless Communications. *IEEE Journal on Selected Areas in Communications*, pages 1451–1458, October 1998.

- [4] A. Naguib, N. Seshadri, and A.R. Calderbank. Increasing Data Rate over Wireless Channels. *IEEE Signal Processing Magazine*, pages 76–92, May 2000.
- [5] T. Rappaport. *Wireless Communications*. IEEE Press, 1996.
- [6] V. Tarokh, H. Jafarkhani, and A.R. Calderbank. Space-Time Block Codes from Orthogonal Designs. *IEEE Transactions on Information Theory*, pages 1456–1467, July 1999.
- [7] P. Stoica and E. Lindskog. Space-Time Block-Coding for Channels with Intersymbol Interference. In *Thirty-Fifth Asilomar Conference on Signals, Systems, and Computers*, October 2001.
- [8] V. Tarokh, A. Naguib, N. Seshadri, and A.R. Calderbank. Space-Time Codes for High Data Rate Wireless Communication : Performance Criteria in the Presence of Channel Estimation Errors, Mobility, and Multiple Paths. *IEEE Transactions on Communications*, pages 199–207, February 1999.
- [9] A. Naguib, V. Tarokh, N. Seshadri, and A.R. Calderbank. A Space-Time Coding Modem for High-Data-Rate Wireless Communications. *IEEE Journal on Selected Areas in Communications*, pages 1459–1477, October 1998.
- [10] N. Seshadri and J. Winters. Two Signaling Schemes for Improving the Error Performance of Frequency-Division-Duplex (FDD) Transmission Systems Using Transmitter Antenna Diversity. In *Vehicular Technology Conference (VTC)*, pages 508–511, 1993.
- [11] Texas Instruments. Space-Time Block Coded Transmit Antenna Diversity for WCDMA. SMG2 document 581/98, submitted October 1998.
- [12] TIA 45.5 Subcommittee. The CDMA 2000 Candidate Submission. Draft, June 1998.
- [13] V. Tarokh, H. Jafarkhani, and A.R. Calderbank. Space-Time Block Coding for Wireless Communications : Performance Results. *IEEE Journal on Selected Areas in Communications*, pages 451–460, March 1999.
- [14] G.D. Forney Jr. Maximum-Likelihood Sequence Estimation of Digital Sequences in the Presence of Intersymbol Interference. *IEEE Transactions on Information Theory*, 18(3):363–378, May 1972.
- [15] W. Younis and N. Al-Dhahir. Joint Prefiltering and MLSE Equalization of Space-Time-Coded Transmissions over Frequency-Selective Channels. *IEEE Transactions on Vehicular Technology*, pages 144–154, January 2002.

- [16] V. Franz and J. Anderson. Concatenated Decoding with a Reduced-Search BCJR Algorithm. *IEEE Journal on Selected Areas in Communication*, pages 186–195, February 1998.
- [17] L. Bahl, J. Cocke, F. Jelinek, and J. Raviv. Optimal Decoding of Linear Codes for Minimizing Symbol Error Rate. *IEEE Transactions on Information Theory*, 20:284–287, March 1974.
- [18] C. Fragouli, N. Al-Dhahir, S. Diggavi, and W. Turin. Prefiltered Space-Time M-BCJR Equalizer for Frequency-Selective Channels. *IEEE Transactions on Communications*, May 2002.
- [19] J. Hagenauer and P. Hoeher. A Viterbi Algorithm with Soft-Decision Outputs and its Applications. In *Global Telecommunications Conference*, pages 47.1.1–47.1.7, November 1989.
- [20] W. Van Etten. Maximum Likelihood Receiver for Multiple Channel Transmission Systems. *IEEE Transactions on Communications*, pages 276–283, February 1976.
- [21] A. Naguib and N. Seshadri. MLSE and Equalization of Space-Time Coded Signals. In *VTC-Spring*, pages 1688–1693, May 2000.
- [22] N. Al-Dhahir. FIR Channel-Shortening Equalizers for MIMO ISI Channels. *IEEE Trans. Communications*, 50:213–218, February 2001.
- [23] A. Duel-Hallen and C. Heegard. Delayed Decision-Feedback Sequence Estimation. *IEEE Transactions on Communications*, pages 428–436, May 1989.
- [24] G. Bauch and N. Al-Dhahir. Iterative Equalization and Decoding with Channel Shortening Filters for Space-Time Coded Modulation. In *VTC Fall*, pages 1575–1582, 2000.
- [25] D. Agrawal, V. Tarokh, A. Naguib, and N. Seshadri. Space-Time Coded OFDM for High Data-Rate Wireless Communication over Wideband Channels. In *VTC*, pages 2232–2236, May 1998.
- [26] N. Al-Dhahir, A. Naguib, and A.R. Calderbank. Finite-Length MIMO Decision-Feedback Equalization for Space-Time Block-Coded Signals over Multipath Fading Channels. *IEEE Transactions on Vehicular Technology*, pages 1176–1181, July 2001.
- [27] H. Viswanathan. Equalization of Space-Time Coded Multi-Antenna Systems. In *Thirty-Eighth Annual Allerton Conference on Communications, Control, and Computing*, pages 658–667, October 2000.

- [28] M. Eyuboglu and S. Qureshi. Reduced-State Sequence Estimation for Coded Modulation of Inter-symbol Interference Channels. *IEEE Journal on Selected Areas in Communications*, pages 989–999, August 1999.
- [29] E. Lindskog and A. Paulraj. A Transmit Diversity Scheme for Delay Spread Channels. In *International Conference on Communications (ICC)*, pages 307–311, June 2000.
- [30] S. Weinstein and P. Ebert. Data Transmission by Frequency-Division Multiplexing Using the Discrete Fourier Transform. *IEEE Trans. on Communications*, 19(5):628–634, October 1971.
- [31] Z. Liu, G. Giannakis, A. Scaglione, and S. Barbarossa. Decoding and Equalization of Unknown Multipath Channels Based on Block Precoding and Transmit-Antenna Diversity. In *Asilomar Conf on Signals, Systems, and Computers*, pages 1557–1561, 1999.
- [32] S. Zhou and G. Giannakis. Space-Time Coded Transmissions with Maximum Diversity Gains over Frequency-Selective Multipath Fading Channels. In *Globecom*, pages 440–444, November 2001.
- [33] H. Sari, G. Karam, and I. Jeanclaude. Transmission Techniques for Digital Terrestrial TV Broadcasting. *IEEE Communications Magazine*, pages 100–109, February 1995.
- [34] Z. Wang and G. Giannakis. Linearly Precoded or Coded OFDM Against Wireless Channel Fades ? In *SPAWC*, pages 267–270, March 2001.
- [35] H. Sari, G. Karam, and I. Jeanclaud. An Analysis of Orthogonal Frequency Division Multiplexing for Mobile Radio Applications. In *VTC*, pages 1635–1639, 1994.
- [36] T. Pollet, M. Van Bladel, and M. Moeneclaey. BER Sensitivity of OFDM Systems to Carrier Frequency Offset and Wiener Phase Noise. *IEEE Transactions on Communications*, pages 191–193, Feb/Mar/April 1995.
- [37] M.V. Clark. Adaptive Frequency-Domain Equalization and Diversity Combining for Broadband Wireless Communications. *IEEE Journal on Selected Areas in Communications*, pages 1385–1395, October 1998.
- [38] N. Al-Dhahir. Single-Carrier Frequency-Domain Equalization for Space-Time Block-Coded Transmissions over Frequency-Selective Fading Channels. *IEEE Communications Letters*, pages 304–306, July 2001.

- [39] G. Kaleh. Channel Equalization for Block Transmission Systems. *IEEE Journal on Selected Areas in Communications*, pages 110–121, January 1995.
- [40] SC FDE PHY Layer Sys. Proposal for Sub 11 GHz BWA. <http://www.ieee802.org/16/tg3/contrib/802163p-0131r2.pdf>.
- [41] S. Diggavi, N. Al-Dhahir, A. Stamoulis, and A.R. Calderbank. Differential Space-Time Transmission for Frequency-Selective Channels. *to appear in IEEE Communications Letters*, 2002.
- [42] S. Crozier, D. Falconer, and S. Mahmoud. Least Sum of Squared Errors (LSSE) Channel Estimation. *IEE Proc. - Part F*, pages 371–378, August 1991.
- [43] D. Chu. Polyphase Codes with Good Periodic Correlation Properties. *IEEE Transactions on Information Theory*, IT-18:531–532, July 1972.
- [44] C. Fragouli, N. Al-Dhahir, and W. Turin. Reduced-Complexity Training Schemes for Multiple-Antenna Broadband Transmissions. In *WCNC*, March 2002.
- [45] C. Fragouli, N. Al-Dhahir, and W. Turin. Finite-Alphabet Constant-Amplitude Training Sequences for Multiple-Antenna Broadband Transmissions. In *ICC*, April 2002.
- [46] J.M. Cioffi and G. Dudevoir and M.V. Eyuboglu and G.D. Forney, Jr. Minimum Mean-Square-Error Decision Feedback Equalization and Coding - Parts I and II. *IEEE Transactions on Communications*, 43:2582–2604, October 1995.

Equalization Scheme	SNR (dB) at BER = $10^{-3}$	Receiver Complexity (per block)
Full BCJR-MAP	21.3	4096 states (each direction)
Prefiltered M-BCJR	23.1	16 states (each direction) 8-tap prefilter (each direction)
Prefiltered DDFSE	23.6	64 states & 32-tap prefilter

Table I. Performance and Complexity Comparison Summary between the Equalization Schemes for the 8-State 8-PSK STTC over the TU EDGE Channel

Equalization Scheme	SNR (dB) at BER = $10^{-3}$	Receiver Complexity (per block)
Full BCJR-MAP	21.3	512 states (each direction) & 20-tap WMF
TR-STBC	22.2	20-tap WMF & 3 feedback taps
FDE-STBC	24.2	Size-64 FFT/IFFT & 64-tap FDE
OFDM-STBC	26.5	Size-64 FFT & 64-tap FDE

Table II. Performance and Complexity Comparison Summary between the Alamouti-Type STBC Equalization Schemes over the TU EDGE Channel Assuming 8-PSK Modulation and Block Size of 64

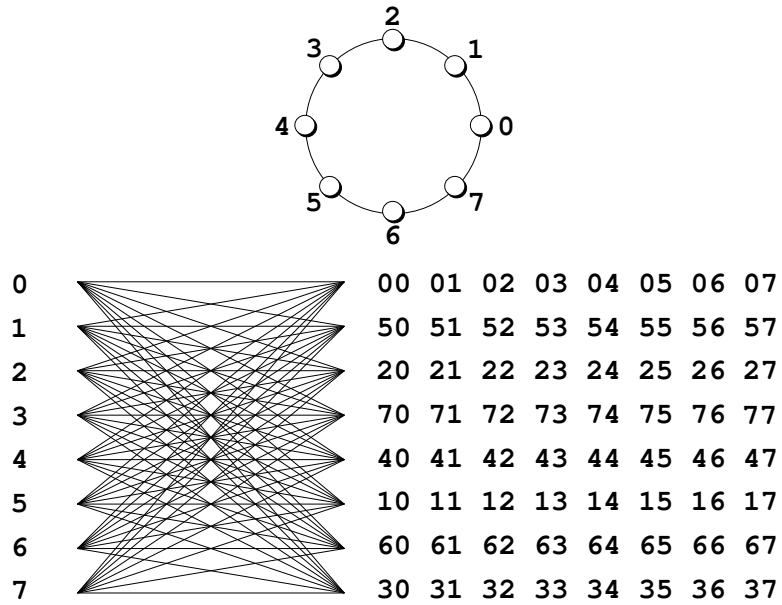


Fig. 1. 8-State 8-PSK Space-Time Trellis Code with Two Transmit Antennas and a Spectral Efficiency of 3 bits/sec/Hz

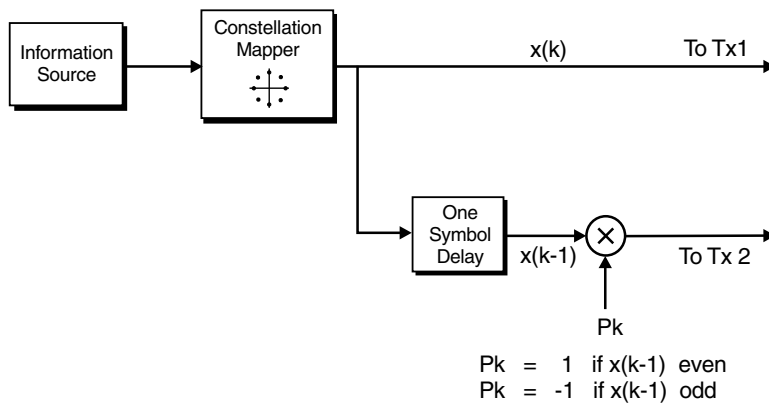


Fig. 2. Equivalent Encoder Model for 8-State 8-PSK Space-Time Trellis Code with Two Transmit Antennas

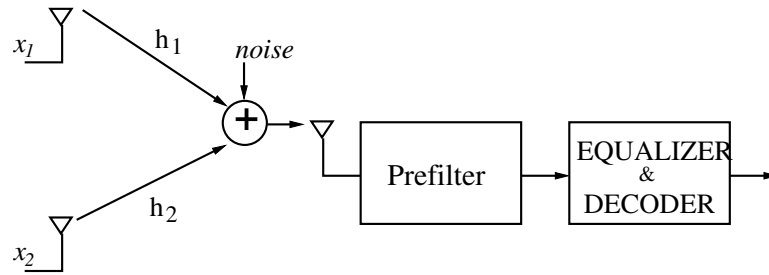


Fig. 3. Receiver Structure for STTC Joint Equalization/Decoding with Two Transmit and One Receive Antennas

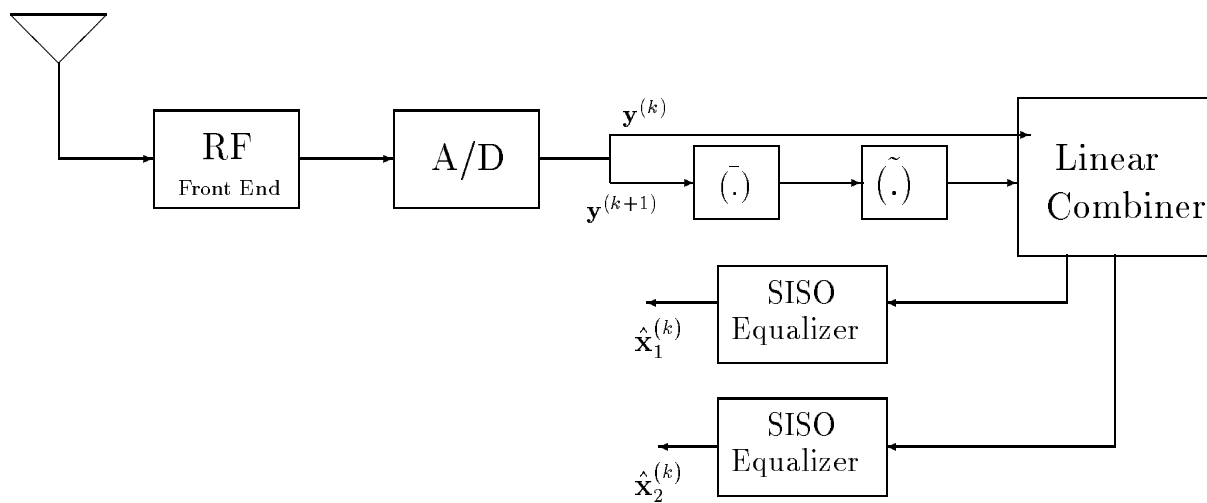


Fig. 4. TR-STBC Receiver Block Diagram. The Operations  $(\bar{\cdot})$  and  $(\tilde{\cdot})$  Denote Complex Conjugation and Time Reversal, Respectively

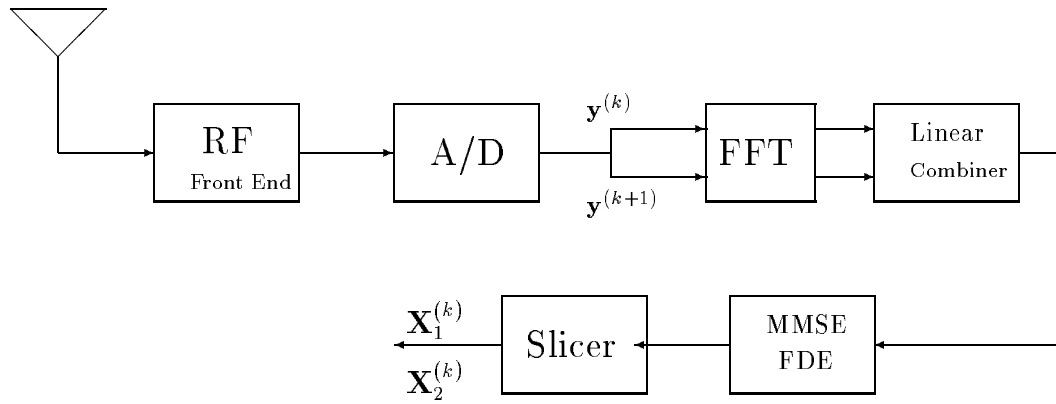


Fig. 5. OFDM-STBC Receiver Block Diagram

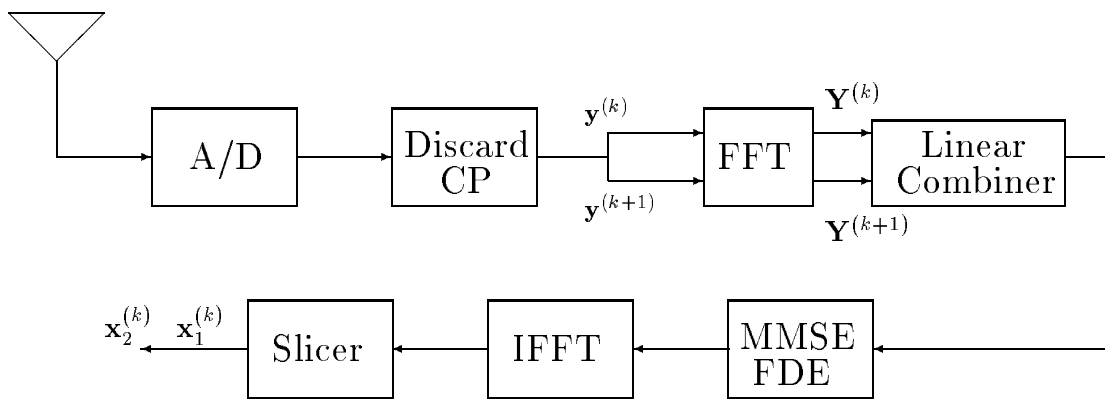


Fig. 6. FDE-STBC Receiver Block Diagram

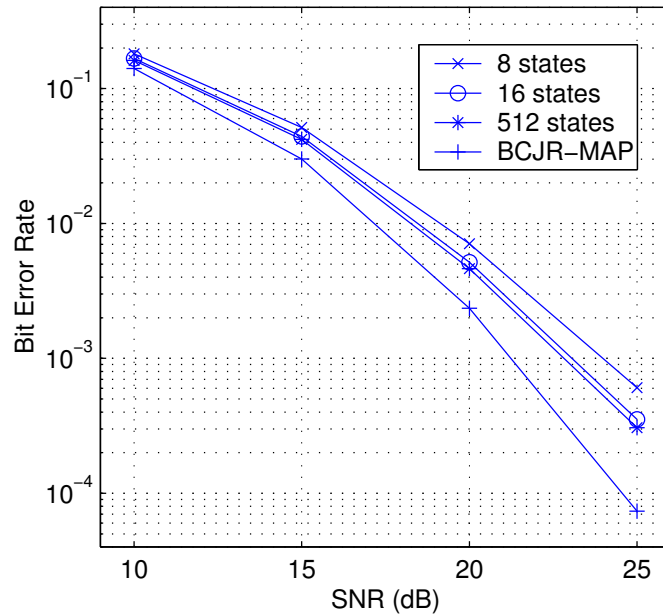


Fig. 7. BER Performance of 2-Transmit 1-Receive 8-State 8-PSK STTC with Prefiltered M-BCJR Equalizer as a function of  $M$  (the Number of Active States). The performance of a 4096-State Full BCJR-MAP Equalizer is Shown as a Benchmark

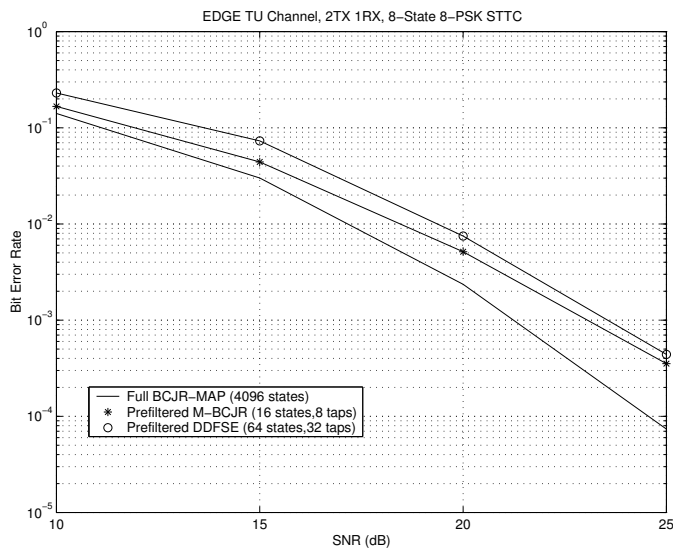


Fig. 8. BER Performance of 2-Transmit 1-Receive 8-State 8-PSK STTC with Prefiltered 64-State DDFSE, Prefiltered 16-State M-BCJR, and Full BCJR-MAP Equalizers

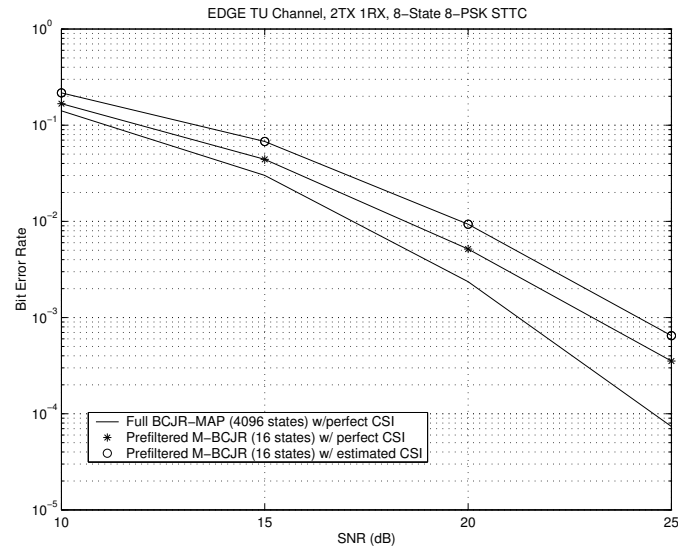


Fig. 9. BER Performance of 2-Transmit 1-Receive 8-State 8-PSK STTC with Prefiltered 16-State M-BCJR with Perfect and Estimated CSI. Full BCJR-MAP Equalizer Performance Shown as BER Lower Bound

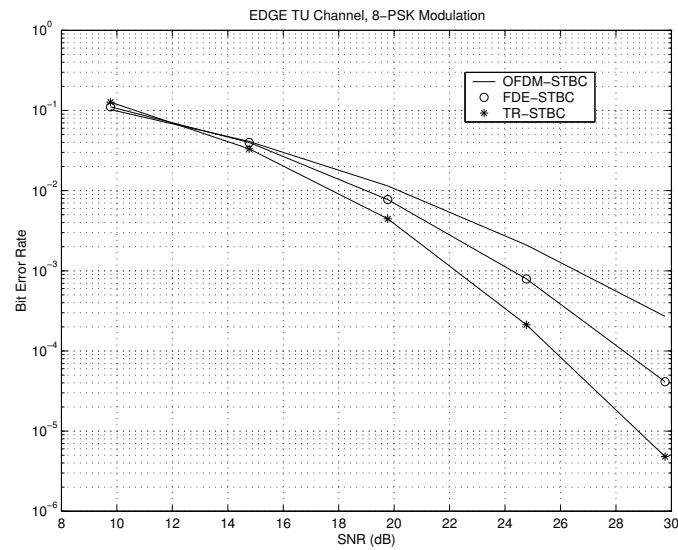


Fig. 10. BER Performance of 2-Transmit 1-Receive OFDM-STBC, FDE-STBC, and TR-STBC. For OFDM-STBC and FDE-STBC, a Size-64 FFT is Assumed. For TR-STBC, An Ideal Whitened Matched Filter Front End and a 3-Tap Feedback Filter are Assumed

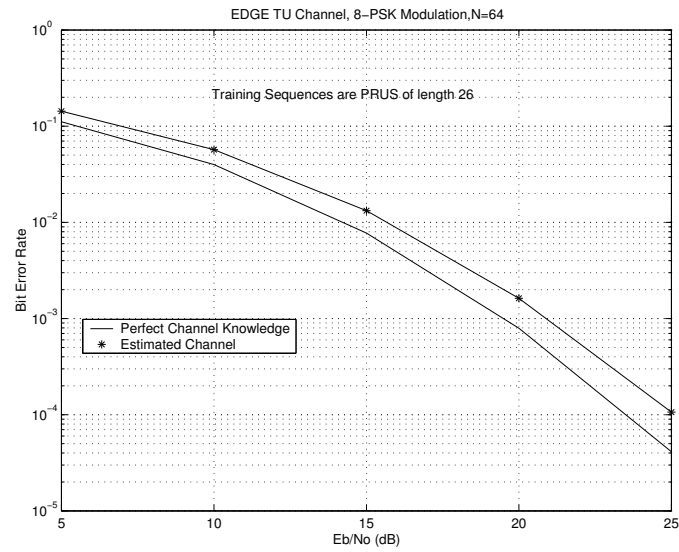


Fig. 11. Effect of Channel Estimation on Performance of SC FDE-STBC

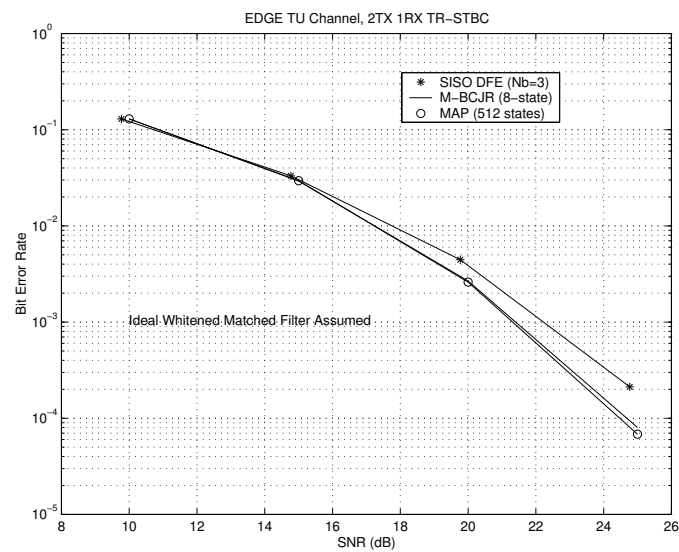


Fig. 12. BER Performance of 2-Transmit 1-Receive TR-STBC with 512-State Full BCJR-MAP, 8-State M-BCJR and SISO MMSE-DFE with  $N_b = 3$  feedback taps. An Ideal Whitened Matched Filter Front End is Assumed